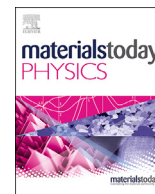




Contents lists available at ScienceDirect

Materials Today Physics

journal homepage: <https://www.journals.elsevier.com/materials-today-physics>

Graphitic carbon nitride nanosheets for microwave absorption

M. Green ^a, Z. Liu ^b, R. Smedley ^a, H. Nawaz ^a, X. Li ^{c, **}, F. Huang ^{b, ***}, X. Chen ^{a, *}^a Department of Chemistry, University of Missouri – Kansas City, MO 64110, USA^b State Key Laboratory of High Performance Ceramics and Superfine Microstructure, Shanghai Institute of Ceramics, Chinese Academy of Sciences, Shanghai 200050, PR China^c College of Forestry and Landscape Architecture, Key Laboratory of Energy Plants Resource and Utilization, Ministry of Agriculture, Key Laboratory of Biomass Energy of Guangdong Regular Higher Education Institutions, South China Agricultural University, Guangzhou, 510642, PR China

ARTICLE INFO

Article history:

Received 17 April 2018

Received in revised form

16 June 2018

Accepted 28 June 2018

Keywords:

2 Dimensional materials

Electromagnetic irradiation

Light-matter interaction

Reflection loss

Interference

ABSTRACT

In this study, we have demonstrated for the first time that the graphitic carbon nitride (g-C₃N₄) nanosheets can possess interesting microwave absorption performance. A large reflection loss (RL) value of −36.1 dB has been demonstrated, corresponding to absorption efficiency over 99.9%. Meanwhile, we have also elucidated the independent contributions of the permittivity and permeability to the microwave absorption. Without the contribution of the electrical or magnetic relaxations, the microwave absorption efficiency decreases. Specifically, the microwave absorption performance decreases much faster without the contribution of the magnetic relaxation than without the contribution of the electrical relaxation. Therefore, the magnetic relaxation in g-C₃N₄ nanosheets has a large role in their microwave absorption. The origins of those relaxations can be traced back to the dipole rotation and magnetic domain resonance inside the materials. In addition, we have also proposed a macroscopic interference model for the microwave absorption behavior of the g-C₃N₄ nanosheets, so that the frequency to reach maximum RL can be precisely predicted given the thickness of the g-C₃N₄ nanosheet absorber.

© 2018 Elsevier Ltd. All rights reserved.

Introduction

Microwave absorbing materials have widely studied for many applications such as wireless communications and antiradar detection [1–3]. For example, they are used to reduce the electromagnetic interference in many electronics and to reduce the radar signature of aircraft, ships, and tanks. So far, various materials and composites have been investigated, such as graphite [4], graphene [2,5], carbon nanotubes (CNTs) [6,7], carbon fiber [8], conducting polymers [9,10], Fe₂O₃ [11], Fe₃O₄ [12], MnO₂ [13], ZnO [14,15], TiO₂ [3,16,17], BaFe₁₂O₁₉ [18], BaTiO₃ [19,20], SrFe₁₂O₁₉ [21], SiC [22], SiCN [23], Co₂P [24], FeP [25], etc. The main mechanisms for microwave absorption are believed to be from the dielectric and magnetic losses inside the materials. For example, the broadband, high-performance microwave absorption in light-weighted, compressible graphene foam has been attributed to the

polarization relaxation of defects or π -electron and interfacial polarization between graphene and other materials [2]. The microwave absorption enhancement of Ni-coated CNTs/epoxy composites is assigned to the dielectric and magnetic losses, while the microwave absorption of Ag nanowire-filled CNTs/epoxy composites is due to the dielectric loss rather than magnetic loss [26]. The microwave absorption of conducting polymers such as polypyrrole, polyaniline, and poly(3-octylthiophene) are caused by the dielectric relaxation in the materials and the interfaces [9]. The enhanced microwave absorption properties of polyaniline with the addition of a suitable amount Fe₂O₃ nanoparticles are accredited to the simultaneous adjusting of dielectric loss and magnetic loss [27]. The shape-dependent microwave absorption properties of MnO₂ with hollow urchin-like nanostructures and the tetragonal nanorod clusters are ascribed to the proper electromagnetic impedance matching [13]. Similar conclusion is drawn in microwave absorption of porous hollow ZnO as well [28]. On the other hand, enhanced microwave absorption performances of hydrogenated TiO₂ [13,16,17], ZnO [15], and BaTiO₃ [20] nanoparticles have been proposed to be from the perturbation of the crystalline structure to introduce partially crystalline phases in changing the dielectric properties. The excellent microwave absorption performance of

* Corresponding author.

** Corresponding author.

*** Corresponding author.

E-mail addresses: xinliscou@yahoo.com (X. Li), huangfq@mail.sic.ac.cn (F. Huang), chenxiaobo@umkc.edu (X. Chen).

Co₂P and FeP nanoparticles has been suggested due to the good coupling between the dielectric and magnetic relaxations in the asymmetric polar lattice and the possible magnetic Co²⁺ and Co⁺ domains in the nanoparticles [24,25]. The microwave absorption in SiC nanoparticles [29] and porous SiCN ceramics [23] has been credited to the dipole relaxation in vacancies and interfaces. Despite of these progresses and the general explanation of the microwave absorption with the dipole rotation and magnetic resonance mechanisms, there lacks of a general model to explain the phenomena that have been observed in almost all the materials in that the frequency of the microwave absorption varies with the thickness of the absorber which is somehow different from what we normally see in optical absorption, for example, ultraviolet–visible (UV–vis) light absorption, where the absorbance increases but the peak's frequency does not change with the concentration or the length of the absorber. Meanwhile, although dipole rotations and magnetic domain resonance are commonly invoked to explain the microwave absorption performance, however, their roles have not yet been explicitly revealed.

In this study, we report for the first time the microwave absorption properties of g-C₃N₄ nanosheets which have been recently widely studied as attractive photocatalysts [30–42]. A large reflection loss (RL) value of –36.1 dB is obtained, with an over 99.9% absorption efficiency. The peak frequency (f_{peak}) can be precisely predicted given the thickness (d) of the absorber. The microwave absorption performance are analyzed in terms of the RL f_{peak} , reflection loss peak value (RL_{peak}), and the critical RL peak width (Δf_{10}), and their relationships with the thickness of the absorber (d). Here, the RL of –10 dB is used as a 'critical value', as in it indicates a 90% threshold for the incident microwave electromagnetic field to be effectively unreflected for signal detection. Δf_{10} means the frequency region within which the RL is more negative than –10 dB. Apparently, it is the effective microwave shielding frequency range. The contributions of the permittivity and permeability to microwave absorption performance are evaluated. Specifically, the microwave absorption efficiency decreases much faster without the contribution of the magnetic relaxation than without the contribution of the electrical relaxation. These effects can be traced back to the dipole rotation and magnetic domain resonance inside the g-C₃N₄ nanosheets that induce the permittivity and permeability properties. We have also proposed a macroscopic interference model to explain the microwave absorption behavior of the g-C₃N₄ nanosheets with the change of the thickness of the absorber.

Materials and methods

The g-C₃N₄ nanosheets were prepared by thermal condensation of melamine at elevated temperatures. Melamine was purchased from ACROS ORGANICS. In a typical synthesis, 10.0 g of melamine was heated at 550 °C for 4 h in air in a small crucible with cap on. After it cooled down to room temperature, it was grinded into fine powder to get g-C₃N₄ nanosheets. The crystal structure of the g-C₃N₄ nanosheets was examined on a Rigaku Miniflex X-ray diffractometer (XRD) with a Cu K α ($\lambda = 0.15418$ nm) radiation source. A suitable amount of the sample was pasted carefully into a thin layer on an amorphous silicon substrate for the XRD measurement. The UV–vis absorption spectrum was collected with an Agilent Cary 60 UV–Vis spectrometer with a fiber optical reflectance unit using the diffusive reflectance method. MgO powder was used as the reference material. The Fourier transform infrared (FTIR) spectrum was collected on a Thermo-Nicolet iS10 FTIR spectrometer equipped with an attenuated total reflectance (ATR) unit where the g-C₃N₄ nanosheets were pressed onto the ZnSe crystal of the ATR unit. The Raman spectrum was collected on an

EZRaman-N benchtop Raman spectrometer with the excitation wavelength of 785 nm. The spectrum range was from 100 cm^{–1} to 3100 cm^{–1}. The spectrum collection time was 4 s and was averaged over three measurements to improve the signal-to-noise ratio. The transmission electron microscopy (TEM) measurements were performed on a FEI Tecnai F200 TEM instrument with an electron accelerating voltage of 200 kV. A few drops of g-C₃N₄ nanosheets dispersed in water were dropped onto a thin holey carbon film, and dried overnight before TEM measurement. The surface chemical bonding and valence band information of the samples was obtained with X-ray photoelectron spectroscopy (XPS) on a PHI 5400 XPS system equipped with a conventional (non-monochromatic) Al anode X-ray source with K α radiation. Small amount of the g-C₃N₄ nanosheets were pressed onto conductive carbon tape for XPS measurements. The binding energies from the samples were calibrated, with respect to the C 1s peak, from the carbon tape at 284.6 eV. The scanning electron microscopy (SEM) image and the energy-dispersive X-ray spectroscopy (EDX) measurement were conducted on a Vegas 3 Tescan SEM instrument equipped with a Bruker EDX unit. The complex permittivity and permeability were measured at the frequency range of 1.0–18.0 GHz using an HP8722ES network analyzer with small ring-shape samples containing 60 wt% g-C₃N₄ nanosheets dispersed in paraffin wax, which was cast into a ring mold with a thickness of 1.0–4.0 mm, an inner diameter of 3.0 mm, and an outer diameter of 7 mm. The thickness of the pellet was carefully controlled by polishing after the pellet was prepared. The measurements were performed at room temperature.

Results and discussion

The formation of g-C₃N₄ nanosheets was believed to be based on the polymerization of melem building blocks. Fig. 1A shows the XRD pattern of the C₃N₄ nanosheets. The XRD pattern had two distinct peaks at 2θ of 13.08 and 27.52° the hexagonal phase of polymeric g-C₃N₄ (JCPDS #87-1526) [40–44]. The strong peak at 27.52° was related to interlayer stacking of the (002) melem planes, and the peak at 12.8° was attributed to the (100) planes corresponding to inplane ordering of the nitrogen-linked heptazine units [40–43]. The peak at 18.04 was attributed to the (310) plane of the polymeric g-C₃N₄ [44]. The interlayer distance of the (002) planes and between the (100) planes calculated were of 0.32 and 0.69 nm for d_{002} and d_{100} , respectively, both close to their theoretical values of 0.34 and 0.73 nm, respectively. The crystallite domain size (L) was calculated according to the Scherrer's equation for the full width at half maximum intensity (FWHM, β) of a diffraction peak $\beta(2\theta)$: $L = K\lambda/\beta(2\theta)\cos\theta$ where λ is the wavelength of the X-rays, θ is the Bragg's angle and K is a constant equal to 0.94 for cube or 0.89 for spherical crystallites [40–45]. In this study K was rounded to 0.9 for simple estimation. The average g-C₃N₄ crystallite size was estimated with Scherrer equation from FWHM of the (002) diffraction peaks at of 8.0 nm. The XRD pattern was consistent with the findings of pure g-C₃N₄ nanosheets in the literature [46–48].

Fig. 1B displays the diffusive UV–vis absorption spectrum. It showed a long-tail absorption from 635.0 to 455.1 nm and a large band absorption below 455.1 nm. The optical bandgap was estimated near 2.73 eV, calculated from the intersection of the long-tail and band absorption at 455.1 nm. The bandgap transition energy E_g was also estimated using the Tauc's equation: $eh\nu = C(h\nu - E_g)^p$, where ϵ is the molar extinction coefficient, which can be obtained from the Beer–Lambert's law, $h\nu$ is the energy of incident photons, C is a constant, E_g is bandgap energy of the material, and p depends on the type of transition [36–42]. For direct semiconductors like g-C₃N₄ $p = 1/2$. The E_g was around 2.92 eV with this method from the

Download English Version:

<https://daneshyari.com/en/article/8918387>

Download Persian Version:

<https://daneshyari.com/article/8918387>

[Daneshyari.com](https://daneshyari.com)